Bol. Soc. Paran. Mat.
©SPM – E-ISSN-2175-1188
SPM: www.spm.uem.br/bspm

(3s.) **v. 2026 (44) 2** : 1–23.
ISSN-0037-8712
doi:10.5269/bspm.78620

Qualitative Analysis of Mpox Transmission Model Incorporating Vaccination And Quarantine Measures

Ibrar Ul Haq, Imtiaz Ahmad, Nigar Ali, Nasro Min-Allah, Amna, S. Islam, Ishtiaq Ali

ABSTRACT: A deterministic six-compartmental model has been built to explain the transmission dynamics of MPox. The population has been divided into six epidemiological classes: susceptible $S(t)$, exposed $E(t)$, infected $I(t)$, vaccinated $V(t)$, quarantined $Q(t)$, and recovered $R(t)$. Control measures like vaccination and quarantine have been included, and natural and disease-induced mortality have been taken into account. The boundedness and positivity of the model solutions have been proven to guarantee well-posedness in a biologically reasonable region. The basic reproduction number R_0 has been obtained to represent the threshold dynamics of the system. It has been revealed that for $R_0 < 1$, the disease-free equilibrium is stable and the disease will eventually disappear. Conversely, when $R_0 > 1$, the infection continues to circulate in the population, and the system has a stable endemic equilibrium.Both the equilibria have been demonstrated to exist and be stable for appropriate parametric conditions. Sensitivity analysis has also been carried out to determine the impact of significant epidemiological parameters on R_0. In addition, the possibility of forward bifurcation has been explored, with the implication of potential multiple endemic equilibria when $R_0 < 1$. Numerical simulations have been carried out to illustrate the qualitative dynamics of the system.

Keywords: MPox, compartmental model, basic reproduction number, forward bifurcation, mathematical epidemiology.

Contents

2020 *Mathematics Subject Classification:* 92D30.
Submitted August 25, 2025. Published March 14, 2026

1. Introduction

Mpox, formerly known as monkeypox, is a zoonotic disease caused by the monkeypox virus (MPXV), a member of the Orthopoxvirus genus. Historically endemic to Central and West Africa, Mpox has re-emerged as a global health concern with outbreaks reported in non-endemic countries since 2022 [1]. The World Health Organization (WHO) declared Mpox a Public Health Emergency of International Concern in August 2024, highlighting its rapid international spread and the emergence of new viral clades [2].

Recent studies have identified the evolution of MPXV into distinct clades, notably Clade I and Clade II, with Clade I associated with higher virulence and mortality rates [3]. The emergence of Clade Ib, characterized by increased transmissibility and potential resistance to existing antiviral treatments, underscores the need for enhanced surveillance and diagnostic capabilities [4].

Traditional diagnostic methods for Mpox, such as polymerase chain reaction (PCR) testing, require specialized laboratory infrastructure, which may not be readily available in resource-limited settings [5]. This limitation hampers timely diagnosis and containment efforts, particularly in regions with limited healthcare resources.

To address these challenges, recent research has explored the application of artificial intelligence (AI) and machine learning (ML) techniques for the detection and diagnosis of Mpox. For instance, Kularathne et al. developed an AI-driven, on-device screening tool capable of offline operation, achieving high accuracy in Mpox detection [6]. Similarly, Yue et al. proposed a lightweight hybrid network, MpoxMamba, designed for efficient Mpox detection in resource-constrained environments [7].Despite these advancements, there remains a need for models that can effectively integrate multimodal data, including clinical information and skin lesion images, to enhance diagnostic accuracy. Cao et al. introduced MpoxVLM, a vision-language model that combines visual and textual data for improved Mpox diagnosis, demonstrating the potential of multimodal approaches [8]. Estimates of pre-symptomatic in fectiousness vary by study and contact setting (sexual vs non-sexual), therefore our model represents an effective average contribution of E to transmission [28].

The proposed model will incorporate advanced deep learning architectures and be optimized for deployment in low-resource settings, thereby addressing current limitations in Mpox detection and contributing to global containment efforts. our modeling plays a good role to guide healthcare professionals in controlling infectious disease diseases such as Ebola [**?**,**?**], rabies [**?**], COVID [**?**,**?**,**?**], and many more [**?**]. We will analyze the proposed model completely. For this, we will follow [**?**,**?**,**?**]. We have divided this paper into 8 sections. Section 2 is a related model formulation. Section 3 is a quantitative analysis. The bifurcation analysis is carried out in Section 4. Sensitivity, numerical simulations, discussion and conclusion have been discussed in the following sections.

2. Model formulation

Six epidemiological compartments are used to stratify the entire population: susceptible $S(t)$, vaccinated $V(t)$, exposed $E(t)$, infectious $I(t)$, quarantined $Q(t)$, and recovered $R(t)$. The susceptible class recruits individuals at a constant rate (A), and the vaccinated class may lose immunity at a rate of (ν_1) or from recovered(τ). Contact with infectious or exposed people can infect susceptibles at rate $(\beta(I+E)S)$, transfer to the vaccinated class at rate (ρ), or cause them to pass away naturally at rate (μ). People who have had vaccinations may have breakthrough infections or lose their immunity (ν_2). Infected individuals in the incubation phase who either progress to infectious state at a rate of (α) or are quarantined at a rate of (ε_2) comprise the exposed class. Additionally, the rate of vaccination is (ε_1). Infectious people may recover (γ), be placed under quarantine (ζ), pass away spontaneously (μ), or contract an illness (μ_0). When members of the exposed or infected class are placed in the quarantined class, they may recover (δ_1), re-infect others (δ_2), lose their immunity (δ_3), or pass away naturally. Lastly, people who have recovered enter from the infectious and quarantined classes and may move to susceptible or die naturally. The rate of change in each compartment over time is described by a series of ordinary differential equations that control the dynamics of the model. The mathematical model is described by the following system

of differential equations:

$$\begin{cases} \dfrac{dS}{dt} = A + \upsilon_1 V + \delta_3 Q + \tau R - (\beta(I+E) + \rho + \mu)S, \\ \dfrac{dE}{dt} = \beta(I+E)S - (\varepsilon_1 + \varepsilon_2 + \alpha + \mu)E, \\ \dfrac{dI}{dt} = \alpha E + \delta_2 Q + \upsilon_2 V - (\zeta + \gamma + \mu + \mu_0)I, \\ \dfrac{dQ}{dt} = \zeta I + \varepsilon_2 E - (\delta_1 + \delta_2 + \delta_3 + \mu)Q, \\ \dfrac{dV}{dt} = \rho S + \varepsilon_1 E - (\upsilon_1 + \upsilon_2 + \mu)V, \\ \dfrac{dR}{dt} = \gamma I + \delta_1 Q - (\tau + \mu)R \end{cases} \tag{2.1}$$

with initial conditions given by:

$$S(0) > 0, \quad V(0) > 0, \quad E(0) \geq 0, \quad I(0) \geq 0, \quad Q(0) \geq 0, \quad R(0) \geq 0$$

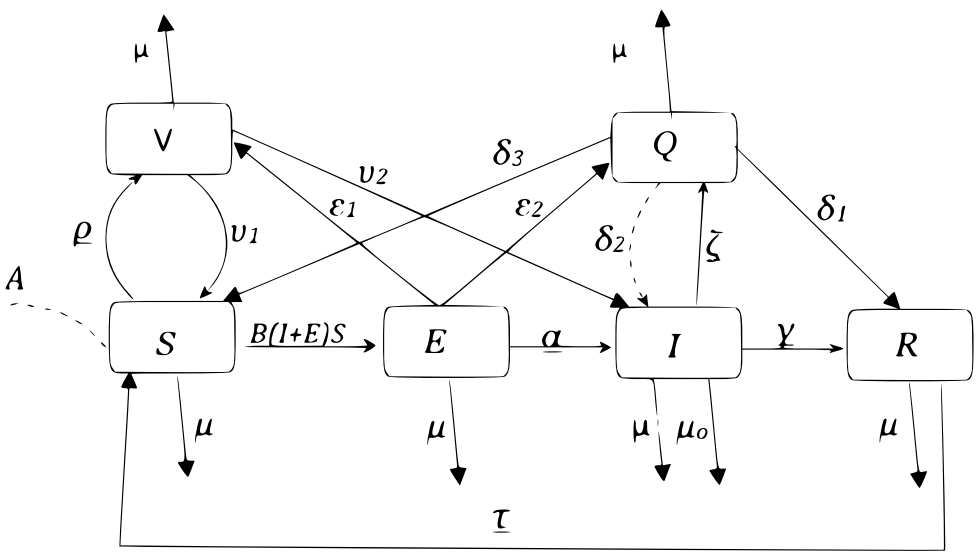

Figure 1: Flow diagram of the Mpox model.

3. Qualitative analysis

3.1. Invariant Region

Theorem 3.1. The solutions of the system remain bounded for all $t \geq 0$, and the closed set Ω defines a biologically feasible and positively invariant region for the system, given by

$$\Omega = \left\{ (S, E, I, Q, V, R) \in \mathbb{R}^6_+ \ : \ S, E, I, Q, V, R \geq 0, \ N(t) \leq \frac{A}{\mu} \right\},$$

where all the variables represent non-negative population classes and the total population size is bounded above by $\frac{A}{\mu}$.

Table 1: Model parameters and their descriptions

Parameter	Description
A	Recruitment rate into the susceptible class
β	Effective contact rate (transmission rate)
μ	Natural death rate
μ_0	Disease-induced death rate for infected individuals
ρ	Rate of vaccination of susceptible individuals
α	Rate of progression from exposed to infected
γ	Recovery rate of infected individuals
ζ	Rate at which infected individuals are quarantined
δ_1	Recovery rate from quarantine
δ_2	Rate at which quarantined individuals become infectious
δ_3	Movement rate of quarantined individuals to susceptible class
τ	Rate at which natural immunity (from recovery) wanes, returning individuals to the susceptible class.
ε_1	Rate at which exposed individuals move to vaccinated class
ε_2	Rate at which exposed individuals move to quarantined class
υ_1	Rate at which vaccine-induced immunity wanes, moving vaccinated individuals back to susceptible
υ_2	Infection rate of vaccinated individuals becoming infected

Proof. Let

$$N(t) = S(t) + E(t) + I(t) + Q(t) + V(t) + R(t)$$

Adding all the equations of system(1) gives:

$$\text{The differential inequality } \frac{dN}{dt} \leq A - \mu N \text{ has the solution:}$$
$$N(t) \leq \left(N(0) - \frac{A}{\mu}\right) e^{-\mu t} + \frac{A}{\mu}$$

Therefore, $\limsup_{t\to\infty} N(t) \leq \frac{A}{\mu}$, which suggests that the entire population is bounded. Additionally, all variables stay non-negative because the system has compartments with non-negative inflows and outflows and begins with non-negative beginning values.Therefore, solutions starting in Ω remain in Ω for all time $t \geq 0$, proving that Ω is positively invariant.

3.2. Existence and uniqueness of the solution

In this subsection,we prove that the solution to system(1) exists and is unique.

Theorem 3.2. The solution of the system (1) with initial conditions, a unique solution exists in $\mathbb{R}^6_+$. That is, the solutions of the state variables S(t), E(t), I(t), V(t), Q(t) and R(t) exist for all $t \in \mathbb{R}_+$ and remain in $\mathbb{R}^6_+$.

Proof: The right-hand side (RHS) of system(1) can be written as:

$$\begin{aligned}
f_1(S,E,I,V,Q,R) &= A + \upsilon_1 V + \delta_3 Q + \tau R - (\beta(I+E) + \rho + \mu)S,\\
f_2(S,E,I,V,Q,R) &= \beta(I+E)S - (\varepsilon_1 + \varepsilon_2 + \alpha + \mu)E,\\
f_3(S,E,I,V,Q,R) &= \alpha E + \delta_2 Q + \upsilon_2 V - (\zeta + \gamma + \mu + \mu_0)I,\\
f_4(S,E,I,V,Q,R) &= \zeta I + \varepsilon_2 E - (\delta_1 + \delta_2 + \delta_3 + \mu)Q,\\
f_5(S,E,I,V,Q,R) &= \rho S + \varepsilon_1 E - (\upsilon_1 + \upsilon_2 + \mu)V,\\
f_6(S,E,I,V,Q,R) &= \gamma I + \delta_1 Q - (\tau + \mu)R,
\end{aligned}$$

Let Ω be the region:

$$\Omega = \left\{ (S(t), E(t), I(t), Q(t), V(t), R(t)) \in \mathbb{R}^6_+ : N(t) \leq \frac{A}{\mu} \right\},$$

where $N(t) = S(t) + E(t) + I(t) + Q(t) + V(t) + R(t)$ is the total population.

Let $U \subset \Omega$ denote the region $|t - t_0| \leq \delta$, $\|x - x_0\| \leq \varepsilon$, where $x = (x_1, x_2, \ldots, x_6)$, and x_0 is the initial condition. Assume that $f(t, x)$ satisfies the Lipschitz condition:

$$\|f(t, x_1) - f(t, x_2)\| \leq K\|x_1 - x_2\|, \quad \text{for all } x_1, x_2 \in U,$$

with $K > 0$ a constant.

This condition is satisfied if the partial derivatives $\left|\frac{\partial f_i}{\partial x_j}\right|$ exist and are bounded in $U \subset \Omega$. For example, for f_1, we have:

$$\left|\frac{\partial f_1}{\partial S}\right| = |-\beta(I + E) - \rho - \mu| < \infty, \quad \left|\frac{\partial f_1}{\partial E}\right| = |\beta S| < \infty, \quad \left|\frac{\partial f_1}{\partial I}\right| = |\beta S| < \infty,$$

$$\left|\frac{\partial f_1}{\partial V}\right| = |\nu_1| < \infty, \quad \left|\frac{\partial f_1}{\partial Q}\right| = |\delta_3| < \infty, \quad \left|\frac{\partial f_1}{\partial R}\right| = |\tau| < \infty$$

Similar arguments apply for $f_2, f_3, \ldots, f_6$. All the partial derivatives $\left|\frac{\partial f_i}{\partial x_j}\right|$ exist and are continuous and bounded in $U \subset \Omega$.

Consequently, the function $f(t, x)$ satisfies the Lipschitz condition, and the system (1) admits unique local solution according to the Picard–Lindelöf Theorem. The local solution extends to a global one when the solution stays in a compact region of $\mathbb{R}^6_+$ because the whole population $N(t)$ is bounded above by $\frac{A}{\mu}$. Hence, the solution $x(t)$ exists, is unique, and remains in $\mathbb{R}^6_+$ for all $t \geq 0$.

3.3. Positivity of the Solution:

In this sub-section, we establish the positivity of the solutions of model (1) equations.

Theorem 3.3. For all given positive initial values, solutions $S(t), E(t), I(t), V(t), Q(t)$ and $R(t)$ of system (1) are non-negative for $t > 0$.

Proof: Consider the first equation of system (1):

$$\frac{dS(t)}{dt} = A + \upsilon_1 V + \delta_3 Q + \tau R - [\beta(I + E) + \rho + \mu] S(t) \tag{3.1}$$

Neglecting the non-negative input terms gives the inequality:

$$\frac{dS(t)}{dt} + [\beta(I + E) + \rho + \mu] S(t) \geq 0 \tag{3.2}$$

Solving this inequality using the integrating factor method, we multiply both sides by the integrating factor

$$e^{\int_0^t [\beta(I+E)+\rho+\mu] ds}$$

which yields:

$$S(t) \geq S(0) e^{-\int_0^t [\beta(I+E)+\rho+\mu] ds} \tag{3.3}$$

Since $S(0) > 0$ and the exponential term is always positive, we conclude that

$$S(t) > 0, \quad \text{for all } t > 0 \tag{3.4}$$

Similarly, one can verify that $E(t)$, $I(t)$, $V(t)$, $Q(t)$, and $R(t)$ are non-negative for $t > 0$.

3.4. Equilibrium Points:

In this section, we derive the disease-free equilibrium (DFE) and endemic equilibrium for the model.

3.4.1. ***Disease-free equilibrium point:*** The disease-free equilibrium, denoted by P_0, can be obtained as follows;

$$P_0 = (S_0, E_0, I_0, Q_0, V_0, R_0) = \left(\frac{A(\upsilon_1 + \upsilon_2 + \mu)}{(\rho + \mu)(\upsilon_1 + \upsilon_2 + \mu) - \upsilon_1 \rho},\ 0,\ 0, 0, \frac{A\rho}{(\rho + \mu)(\upsilon_1 + \upsilon_2 + \mu) - \upsilon_1 \rho},\ 0 \right)$$

3.4.2. ***Endemic equilibrium point:*** The endemic equilibrium point denoted by P_1 of model (1) can be obtained as follows:

$$P_1 = \begin{pmatrix} S^* = \dfrac{(\varepsilon_1 + \varepsilon_2 + \alpha + \mu)E^*}{\beta(E^* + I^*)} \\ E^* = \frac{\beta I^* S^*}{(\varepsilon_1 + \varepsilon_2 + \alpha + \mu) - \beta S^*} \\ I^* = \dfrac{\alpha E^* + \delta_2 Q^* + \upsilon_2 V^*}{\zeta + \gamma + \mu + \mu_0} \\ Q^* = \dfrac{\zeta I^* + \varepsilon_2 E^*}{\delta_1 + \delta_2 + \delta_3 + \mu} \\ V^* = \dfrac{\rho S^* + \varepsilon_1 E^*}{\upsilon_1 + \upsilon_2 + \mu} \\ R^* = \dfrac{\gamma I^* + \delta_1 Q^*}{\tau + \mu} \end{pmatrix}$$

3.5. Basic Reproduction Number R_0:

Following the next-generation matrix method [3,13]:
We construct the Jacobian matrices at the disease-free equilibrium (DFE):

$$F^* = \begin{bmatrix} \beta S_0 & \beta S_0 & 0 \\ 0 & 0 & 0 \\ 0 & 0 & 0 \end{bmatrix}, \quad V^* = \begin{bmatrix} A' & 0 & 0 \\ -\alpha & B & -\delta_2 \\ -\epsilon_2 & -\zeta & C \end{bmatrix}$$

where

$$A' = \epsilon_1 + \epsilon_2 + \alpha + \mu, B = \zeta + \gamma + \mu + \mu_o, C = \delta_1 + \delta_2 + \delta_3 + \mu$$
$$D = \nu_1 + \nu_2 + \mu, S_0 = \frac{AD}{(\rho + \mu)D - \nu_1 \rho}$$

Now, the next-generation matrix is given by:

$$K = F^* {V^*}^{-1}$$

$$K = \begin{bmatrix} \beta S_0 \left(\dfrac{1}{A'} + \dfrac{C\alpha + \delta_2 \epsilon_2}{A'(BC - \delta_2 \zeta)} \right) & \beta S_0 \cdot \dfrac{C}{(BC - d_2 \zeta)} & \beta S_0 \cdot \dfrac{\delta_2}{(BC - \delta_2 \zeta)} \\ 0 & 0 & 0 \\ 0 & 0 & 0 \end{bmatrix}$$

Finally, the basic reproduction number R_0 is the spectral radius (dominant eigenvalue) of K, which simplifies to:

$$R_0 = \frac{A\beta D}{A'((\rho + \mu)D - \nu_1 \rho)} \left(1 + \frac{C\alpha + \delta_2 \epsilon_2}{(BC - \delta_2 \zeta)} \right)$$

Back substitution gives us:

$$R_0 = \frac{A\beta(\nu_1 + \nu_2 + \mu)}{(\epsilon_1 + \epsilon_2 + \alpha + \mu)((\rho + \mu)(\nu_1 + \nu_2 + \mu) - \rho\nu_1)} \left(1 + \frac{(\delta_1 + \delta_2 + \delta_3 + \mu)\alpha + \delta_2 \epsilon_2}{(\zeta + \gamma + \mu + \mu_o)(\delta_1 + \delta_2 + \delta_3 + \mu) - \delta_2 \zeta} \right)$$

3.6. 3D type simulation:

In figure:2, six three-dimensional surface plots showing the fluctuation of the basic reproduction number R_0 in response to various pairs of model parameters are presented in Figure 2. The top-left plot shows that R_0 increases with both the effective contact rate β and the transition rate ν_1, indicating their positive contribution to disease transmission. An inverse relationship is shown in the top-right plot, where R_0 increases with β but decreases with the recovery rate ν_2. The middle-left plot illustrates that increasing the parameters ϵ_1 and ϵ_2, which may represent control or removal rates, leads to a decrease in R_0, suggesting their effectiveness in reducing disease spread. A similar pattern is observed in the middle-right plot, where higher values of the progression rate α and ϵ_2 result in a reduction of R_0. The negative influence of ν_1 and ϵ_1 on R_0 is further confirmed in the bottom-left plot. Finally, the bottom-right plot shows that increasing both α and ν_2 effectively reduces the value of R_0.

3.7. Stability analysis

In this subsection,we present both local and global asymptotic stabilities of the equilibria of system(1).

3.7.1.Local Stability:

In this subsection we discuss the local stability.

3.4.Theorem. The disease-free equilibrium (DFE) point P_0 of system (1) is locally asymptotically stable if $\mathcal{R}_0 < 1$ and unstable if $\mathcal{R}_0 > 1$.

Proof. Consider the Jacobian matrix at the DFE P_0:

$$J_{P_0} = \begin{pmatrix} -(\rho+\mu) & -\beta S_0 & -\beta S_0 & \delta_3 & \upsilon_1 & \tau \\ 0 & \beta S_0 - Z_1 & \beta S_0 & 0 & 0 & 0 \\ 0 & \alpha & -Z_2 & \delta_2 & \upsilon_2 & 0 \\ 0 & \varepsilon_2 & \zeta & -Z_3 & 0 & 0 \\ \rho & \varepsilon_1 & 0 & 0 & -Z_4 & 0 \\ 0 & 0 & \gamma & \delta_1 & 0 & -Z_5 \end{pmatrix}$$

where:

$$Z_1 = \varepsilon_1 + \varepsilon_2 + \alpha + \mu, \quad Z_2 = \zeta + \gamma + \mu + \mu_0, \quad Z_3 = \delta_1 + \delta_2 + \delta_3 + \mu,$$
$$Z_4 = \upsilon_1 + \upsilon_2 + \mu, \quad Z_5 = \tau + \mu$$

We apply a sequence of elementary row operations and Using Laplace expansion to reduce the matrix:

$$\text{Row operation:} \quad R_1 \leftarrow R_1 - \frac{\tau}{Z_5} R_6$$

$$J_{P_0} = \begin{pmatrix} -(\rho+\mu) & -\beta S_0 & -\beta S_0 + \frac{\gamma\tau}{Z_5} & \delta_3 + \frac{\delta_1\tau}{Z_5} & \upsilon_1 & 0 \\ 0 & \beta S_0 - Z_1 & \beta S_0 & 0 & 0 & 0 \\ 0 & \alpha & -Z_2 & \delta_2 & \upsilon_2 & 0 \\ 0 & \varepsilon_2 & \zeta & -Z_3 & 0 & 0 \\ \rho & \varepsilon_1 & 0 & 0 & -Z_4 & 0 \\ 0 & 0 & \gamma & \delta_1 & 0 & -Z_5 \end{pmatrix}$$

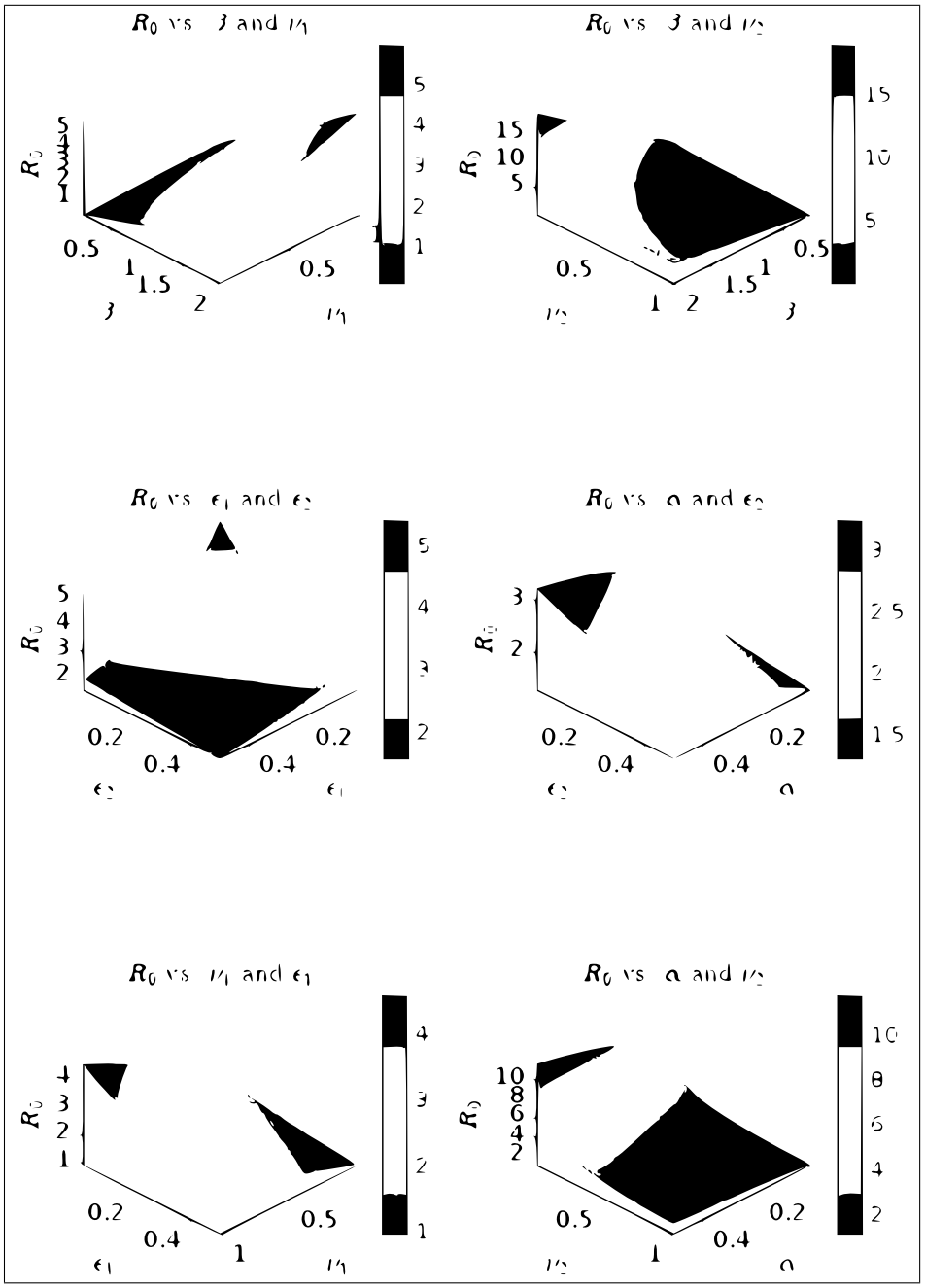

Figure 2: 3D simulation of R_0

Now by applying laplace expansion along C_6, we obtain $\lambda_1 = -Z_5$

$$J_{P_0} = \begin{pmatrix} -(\rho+\mu) & -\beta S_0 & -\beta S_0 + \frac{\gamma\tau}{Z_5} & \delta_3 + \frac{\delta_1\tau}{Z_5} & \upsilon_1 \\ 0 & \beta S_0 - Z_1 & \beta S_0 & 0 & 0 \\ 0 & \alpha & -Z_2 & \delta_2 & \upsilon_2 \\ 0 & \varepsilon_2 & \zeta & -Z_3 & 0 \\ \rho & \varepsilon_1 & 0 & 0 & -Z_4 \end{pmatrix}$$

$$R_5 \leftarrow R_5 + \frac{\rho}{\rho+\mu}R_1$$

$$J_{P_0} = \begin{pmatrix} -(\rho+\mu) & -\beta S_0 & -\beta S_0 + \frac{\gamma\tau}{Z_5} & \delta_3 + \frac{\delta_1\tau}{Z_5} & \upsilon_1 \\ 0 & \beta S_0 - Z_1 & \beta S_0 & 0 & 0 \\ 0 & \alpha & -Z_2 & \delta_2 & \upsilon_2 \\ 0 & \varepsilon_2 & \zeta & -Z_3 & 0 \\ 0 & \varepsilon_1 - \frac{\rho\beta S_0}{\rho+\mu} & \frac{\rho}{\rho+\mu}\left(-\beta S_0 + \frac{\gamma\tau}{Z_5}\right) & \frac{\rho}{\rho+\mu}\left(\delta_3 + \frac{\delta_1\tau}{Z_5}\right) & -Z_4 + \frac{\rho\upsilon_1}{\rho+\mu} \end{pmatrix}$$

By Applying laplace expansion along C_1 we obtain $\lambda_2 = -(\rho+\mu)$,the remaining eigenvalues are the eigenvalues of the matrix

$$J_{p_0} = \begin{pmatrix} \beta S_0 - Z_1 & \beta S_0 & 0 & 0 \\ \alpha & -Z_2 & \delta_2 & \upsilon_2 \\ \varepsilon_2 & \zeta & -Z_3 & 0 \\ \varepsilon_1 - \frac{\rho\beta S_0}{\rho+\mu} & \frac{\rho}{\rho+\mu}\left(-\beta S_0 + \frac{\gamma\tau}{Z_5}\right) & \frac{\rho}{\rho+\mu}\left(\delta_3 + \frac{\delta_1\tau}{Z_5}\right) & -Z_4 + \frac{\rho\upsilon_1}{\rho+\mu} \end{pmatrix}$$

The reduce matrix will have negative eigenvalues iff its trace is negative and its determinant is positive [25].

$$trace(J_{P_0}) = (\beta S_0 - Z_1) - Z_2 - Z_3 - (Z_4 - \frac{\rho\upsilon_1}{\rho+\mu}) < 0$$

$$|J_{p_0}| = \begin{vmatrix} \beta S_0 - Z_1 & \beta S_0 & 0 & 0 \\ \alpha & -Z_2 & \delta_2 & \upsilon_2 \\ \varepsilon_2 & \zeta & -Z_3 & 0 \\ \varepsilon_1 - \frac{\rho\beta S_0}{\rho+\mu} & \frac{\rho}{\rho+\mu}\left(-\beta S_0 + \frac{\gamma\tau}{Z_5}\right) & \frac{\rho}{\rho+\mu}\left(\delta_3 + \frac{\delta_1\tau}{Z_5}\right) & -Z_4 + \frac{\rho\upsilon_1}{\rho+\mu} \end{vmatrix} > 0$$

$$|J_{P_0}| = (\beta S_0 - Z_1)\left[\frac{\rho}{\rho+\mu}\left(-\beta S_0 + \frac{\gamma\tau}{Z_5}\right)\upsilon_2 Z_3 - \frac{\rho}{\rho+\mu}\left(\delta_3 + \frac{\delta_1\tau}{Z_5}\right)\upsilon_2\zeta + \left(-Z_4 + \frac{\rho\upsilon_1}{\rho+\mu}\right)(Z_2Z_3 - \delta_2\zeta)\right]$$
$$-\beta S_0\left[\left(\varepsilon_1 - \frac{\rho\beta S_0}{\rho+\mu}\right)\upsilon_2 Z_3 + \frac{\rho}{\rho+\mu}\left(\delta_3 + \frac{\delta_1\tau}{Z_5}\right)\upsilon_2\varepsilon_2 + \left(-Z_4 + \frac{\rho\upsilon_1}{\rho+\mu}\right)(-\alpha Z_3 - \delta_2\varepsilon_2)\right] > 0$$

$$\begin{aligned} |J_{P_0}| = {} & (\beta S_0 - Z_1)\left[\frac{\rho}{\rho+\mu}\left(-\beta S_0 + \frac{\gamma\tau}{Z_5}\right)\upsilon_2 Z_3 - \frac{\rho}{\rho+\mu}\left(\delta_3 + \frac{\delta_1\tau}{Z_5}\right)\upsilon_2\zeta\right] \\ & - \beta S_0\left[\left(\varepsilon_1 - \frac{\rho\beta S_0}{\rho+\mu}\right)\upsilon_2 Z_3 + \frac{\rho}{\rho+\mu}\left(\delta_3 + \frac{\delta_1\tau}{Z_5}\right)\upsilon_2\varepsilon_2\right] \\ & + Z_1(Z_2Z_3 - \delta_2\zeta)\left(-Z_4 + \frac{\rho\upsilon_1}{\rho+\mu}\right)\left[\frac{\beta S_0}{Z_1} - 1 + \frac{\beta S_0}{Z_1}\cdot\frac{(\alpha Z_3 + \delta_2\varepsilon_2)}{(Z_2Z_3 - \delta_2\zeta)}\right] > 0 \end{aligned}$$

$$\begin{aligned} |J_{P_0}| = {} & (\beta S_0 - Z_1)\left[\frac{\rho}{\rho+\mu}\left(-\beta S_0 + \frac{\gamma\tau}{Z_5}\right)\upsilon_2 Z_3 - \frac{\rho}{\rho+\mu}\left(\delta_3 + \frac{\delta_1\tau}{Z_5}\right)\upsilon_2\zeta\right] \\ & - \beta S_0\left[\left(\varepsilon_1 - \frac{\rho\beta S_0}{\rho+\mu}\right)\upsilon_2 Z_3 + \frac{\rho}{\rho+\mu}\left(\delta_3 + \frac{\delta_1\tau}{Z_5}\right)\upsilon_2\varepsilon_2\right] \\ & + Z_1(Z_2Z_3 - \delta_2\zeta)\left(-Z_4 + \frac{\rho\upsilon_1}{\rho+\mu}\right)(R_0 - 1) > 0 \end{aligned}$$

The determinant will be positive if $R_0 < 1$.It implies that the DFE points are LAS when $R_0 < 1$ otherwise unstable. Local Stability of the Disease-Free Equilibrium (DFE)

Theorem.3.5. The endemic equilibrium point P_1 is locally asymptotically stable whenever $R_0 > 1$, and unstable otherwise.

Proof. The Jacobian matrix of system (1), evaluated at the endemic equilibrium point P_1, is given by

$$J_{P_1} = \begin{pmatrix} -\beta(E^*+I^*)-\rho-\mu & -\beta S^* & -\beta S^* & \delta_3 & \upsilon_1 & \tau \\ \beta(E^*+I^*) & \beta S^* - Z_1 & \beta S^* & 0 & 0 & 0 \\ 0 & \alpha & -Z_2 & \delta_2 & \upsilon_2 & 0 \\ 0 & \varepsilon_2 & \zeta & -Z_3 & 0 & 0 \\ \rho & \varepsilon_1 & 0 & 0 & -Z_4 & 0 \\ 0 & 0 & \gamma & \delta_1 & 0 & -Z_5 \end{pmatrix}$$

To reduce the matrix we apply a sequence of row operations and Laplace expansion.

$$R_1 \leftarrow R_1 + \frac{\tau}{Z_5} R_6$$

$$J_{P_1} = \begin{pmatrix} -\beta(E^*+I^*)-\rho-\mu & -\beta S^* & -\beta S^* + \frac{\tau\gamma}{Z_5} & \delta_3 + \frac{\tau\delta_1}{Z_5} & \upsilon_1 & 0 \\ \beta(E^*+I^*) & \beta S^* - Z_1 & \beta S^* & 0 & 0 & 0 \\ 0 & \alpha & -Z_2 & \delta_2 & \upsilon_2 & 0 \\ 0 & \varepsilon_2 & \zeta & -Z_3 & 0 & 0 \\ \rho & \varepsilon_1 & 0 & 0 & -Z_4 & 0 \\ 0 & 0 & \gamma & \delta_1 & 0 & -Z_5 \end{pmatrix}$$

Expand along C_6

$$J_{P_1} = \begin{pmatrix} -\beta(E^*+I^*)-\rho-\mu & -\beta S^* & -\beta S^* + \frac{\tau\gamma}{Z_5} & \delta_3 + \frac{\tau\delta_1}{Z_5} & \upsilon_1 \\ \beta(E^*+I^*) & \beta S^* - Z_1 & \beta S^* & 0 & 0 \\ 0 & \alpha & -Z_2 & \delta_2 & \upsilon_2 \\ 0 & \varepsilon_2 & \zeta & -Z_3 & 0 \\ \rho & \varepsilon_1 & 0 & 0 & -Z_4 \end{pmatrix}$$

To eliminate the terms υ_1 from row 1 and υ_2 from row 3, the following elementary row operations are applied:

$$R_1 \leftarrow R_1 + \frac{\upsilon_1}{Z_4} R_5, \qquad R_3 \leftarrow R_3 + \frac{\upsilon_2}{Z_4} R_5$$

$$J_{P_1} = \begin{pmatrix} -\beta(E^*+I^*)-\rho-\mu+\frac{\upsilon_1\rho}{Z_4} & -\beta S^* + \frac{\upsilon_1\varepsilon_1}{Z_4} & -\beta S^* + \frac{\tau\gamma}{Z_5} & \delta_3 + \frac{\tau\delta_1}{Z_5} & 0 \\ \beta(E^*+I^*) & \beta S^* - Z_1 & \beta S^* & 0 & 0 \\ \frac{\upsilon_2\rho}{Z_4} & \alpha + \frac{\upsilon_2\varepsilon_1}{Z_4} & -Z_2 & \delta_2 & 0 \\ 0 & \varepsilon_2 & \zeta & -Z_3 & 0 \\ \rho & \varepsilon_1 & 0 & 0 & -Z_4 \end{pmatrix}$$

Expanding along column 5:

$$J_{P_1} = \begin{pmatrix} -\beta(E^*+I^*) - \rho - \mu + \frac{\upsilon_1\rho}{Z_4} & -\beta S^* + \frac{\upsilon_1\varepsilon_1}{Z_4} & -\beta S^* + \frac{\tau\gamma}{Z_5} & \delta_3 + \frac{\tau\delta_1}{Z_5} \\ \beta(E^*+I^*) & \beta S^* - Z_1 & \beta S^* & 0 \\ \frac{\upsilon_2\rho}{Z_4} & \alpha + \frac{\upsilon_2\varepsilon_1}{Z_4} & -Z_2 & \delta_2 \\ 0 & \varepsilon_2 & \zeta & -Z_3 \end{pmatrix}$$

$$det(\lambda I - J_{P_1}) = \begin{vmatrix} \lambda + \beta(E^*+I^*) + \rho + \mu - \frac{\upsilon_1\rho}{Z_4} & \beta S^* - \frac{\upsilon_1\varepsilon_1}{Z_4} & \beta S^* - \frac{\tau\gamma}{Z_5} & -\delta_3 - \frac{\tau\delta_1}{Z_5} \\ -\beta(E^*+I^*) & \lambda - \beta S^* + Z_1 & -\beta S^* & 0 \\ -\frac{\upsilon_2\rho}{Z_4} & -\alpha - \frac{\upsilon_2\varepsilon_1}{Z_4} & \lambda + Z_2 & -\delta_2 \\ 0 & -\varepsilon_2 & -\zeta & \lambda + Z_3 \end{vmatrix} = 0$$

$$f_0\lambda^4 + f_1\lambda^3 + f_2\lambda^2 + f_3\lambda + f_4 = 0$$

where

$$f_0 = 1,$$

$$f_1 = \beta(E^*+I^*) + \rho + \mu - \frac{\upsilon_1\rho}{Z_4} + Z_1 + Z_2 + Z_3,$$

$$\begin{aligned} f_2 = {} & \left(-\beta(E^*+I^*) - \rho - \mu + \frac{\upsilon_1\rho}{Z_4}\right)(\beta S^* - Z_1) + \left(\beta S^* - \frac{\upsilon_1\varepsilon_1}{Z_4}\right)\beta(E^*+I^*) \\ & + \left(-\beta(E^*+I^*) - \rho - \mu + \frac{\upsilon_1\rho}{Z_4}\right)(-Z_2 - Z_3) + \left(\beta S^* - \frac{\tau\gamma}{Z_5}\right)\frac{\upsilon_2\rho}{Z_4} \\ & + (\beta S^* - Z_1)(-Z_2 - Z_3) + Z_2Z_3 - \beta S^*\left(\alpha + \frac{\upsilon_2\varepsilon_1}{Z_4}\right) - \delta_2\zeta, \end{aligned}$$

$$\begin{aligned} f_3 = {} & \left(\delta_3 + \frac{\tau\delta_1}{Z_5}\right)\left[\varepsilon_2\left(\beta S^* - \frac{\tau\gamma}{Z_5}\right) + \zeta\left(\alpha + \frac{\upsilon_2\varepsilon_1}{Z_4}\right)\right] \\ & + \left(\beta(E^*+I^*) + \rho + \mu - \frac{\upsilon_1\rho}{Z_4}\right)(Z_1Z_2 + Z_1Z_3 + Z_2Z_3) \\ & - \left(\beta S^* - \frac{\tau\gamma}{Z_5}\right)\left(\alpha + \frac{\upsilon_2\varepsilon_1}{Z_4}\right)Z_1 - \left(\beta S^* - \frac{\upsilon_1\varepsilon_1}{Z_4}\right)\beta(E^*+I^*)Z_2 \\ & - \left(\beta S^*\cdot\alpha + \frac{\beta S^*\upsilon_2\varepsilon_1}{Z_4}\right)Z_3, \end{aligned}$$

$$f_4 = \left(\delta_3 + \frac{\tau\delta_1}{Z_5}\right)\left[\varepsilon_2\left(\beta S^* - \frac{\tau\gamma}{Z_5}\right) + \zeta\left(\alpha + \frac{\upsilon_2\varepsilon_1}{Z_4}\right)\right]\beta(E^*+I^*)$$

We need to verify the following conditions:

(a) $f_0, f_1, f_2, f_3, f_4 > 0$

(b) $f_1f_2 - f_0f_3 > 0$

(c) $f_1f_2f_3 - f_0f_3^2 - f_1^2f_4 > 0$

Condition (a) is satisfied. Condition (b) and (c) will holds if $f_1f_2 > f_0f_3$ and $f_1f_2f_3 > f_0f_3^2 + f_1^2f_4$ respectively.

The Routh–Hurwitz criterion and the conditions (a) - (c) implies that all the roots of the characteristic equation have negative real parts, which guarantees that the endemic equilibrium point P_1 is locally asymptotically stable (LAS).

3.7.2.Global Stability

In this section, we discuss the global stability.

Theorem.3.6. The disease-free equilibrium point P_0 of system(1) is globally asymptotically stable if $R_0 < 1$.

Proof. We define the Lyapunov function

$$\mathcal{L}(t) = E + aI + bQ,$$

where

$$a = \frac{\beta S_0 Z_3}{Z_2 Z_3 - \delta_2 \zeta}, \quad b = \frac{\beta S_0 \delta_2}{Z_2 Z_3 - \delta_2 \zeta},$$

We now compute the derivative of $\mathcal{L}(t)$ along the solutions of the system:

$$\begin{aligned}\frac{d\mathcal{L}}{dt} &= \frac{dE}{dt} + a\frac{dI}{dt} + b\frac{dQ}{dt} \\ &= \beta S(I+E) - Z_1 E + a\left(\alpha E + \delta_2 Q + \upsilon_2 V - Z_2 I\right) + b\left(\zeta I + \varepsilon_2 E - Z_3 Q\right)\end{aligned}$$

Grouping terms, we obtain:

$$\frac{d\mathcal{L}}{dt} = E\left(\beta S - Z_1 + a\alpha + b\varepsilon_2\right) + I\left(\beta S - aZ_2 + b\zeta\right) + Q\left(a\delta_2 - bZ_3\right) + a\upsilon_2 V$$

Now observe that:

$$a\delta_2 - bZ_3 = 0,$$

$$\beta S - aZ_2 + b\zeta = 0,$$

Thus,

$$\frac{d\mathcal{L}}{dt} = E\left(\beta S - Z_1 + \frac{\beta S_0(Z_3\alpha + \delta_2\varepsilon_2)}{Z_2 Z_3 - \delta_2\zeta}\right) + a\upsilon_2 V$$

So we write:

$$\frac{d\mathcal{L}}{dt} = Z_1 E(R_0 - 1) + a\upsilon_2 V$$

Clearly, if $R_0 < 1$, then $\frac{d\mathcal{L}}{dt} < 0$, except at the DFE where $E = I = Q = 0$. By LaSalle's Invariance Principle, the DFE is globally asymptotically stable.

Theorem.3.7 If $R_0 > 1$, then the endemic equilibrium point $P_1 = (S^*, E^*, I^*, V^*, Q^*, R^*)$ is globally asymptotically stable.

Proof: Let $P_1 = (S^*, E^*, I^*, V^*, Q^*, R^*)$ be the endemic equilibrium of system (1). Define the total population as:

$$Z(t) = S(t) + E(t) + I(t) + V(t) + Q(t) + R(t),$$

and assume that the feasible region is positively invariant and attracting.

We define the Lyapunov function as:

$$H(t) = \frac{1}{2}\left[(S - S^*)^2 + (E - E^*)^2 + (I - I^*)^2 + (V - V^*)^2 + (Q - Q^*)^2 + (R - R^*)^2\right]$$

Clearly, $H : \mathbb{R}^6_+ \to \mathbb{R}$ is continuous and differentiable, and $H(t) = 0$ if and only if $S = S^*, E = E^*, \ldots, R = R^*$. Its derivative along trajectories of the system is:

$$\frac{dH}{dt} = (S - S^*)\frac{dS}{dt} + (E - E^*)\frac{dE}{dt} + (I - I^*)\frac{dI}{dt} + (V - V^*)\frac{dV}{dt} + (Q - Q^*)\frac{dQ}{dt} + (R - R^*)\frac{dR}{dt}$$

Let us define the net population deviation from the endemic point:

$$Z^* = S^* + E^* + I^* + V^* + Q^* + R^*$$

From the model, the total derivative of the population satisfies:

$$\frac{dZ}{dt} = A - \mu Z(t) - \mu_0 I(t)$$

At equilibrium, we have:

$$\frac{dZ^*}{dt} = 0 \Rightarrow A - \mu Z^* - \mu_0 I^* = 0 \Rightarrow Z^* = \frac{A - \mu_0 I^*}{\mu}$$

Then,

$$\frac{dH}{dt} = [Z(t) - Z^*]\frac{dZ}{dt}$$

Substitute in the expression for $\frac{dZ}{dt}$ and Z*:

$$\frac{dH}{dt} = \left(Z - \frac{A - \mu_0 I^*}{\mu}\right)(A - \mu Z - \mu_0 I)$$

$$\frac{dH}{dt} \leq \mu\left(Z - \frac{A}{\mu}\right)\left(\frac{A}{\mu} - Z\right)$$

$$\frac{dH}{dt} = -\mu\left(Z - \frac{A}{\mu}\right)^2 < 0$$

Thus, according to LaSalle's Invariance Principle, the endemic equilibrium P_1 is globally asymptotically stable.

4. Bifurcation Analysis

In this section, we perform the presence of bifurcation and offer a detailed demonstration of forward bifurcation using the Chavez & Song technique [27] and the central manifold theory [26].

Theorem 4.1. The model undergoes a transcritical bifurcation at the disease-free equilibrium point P_0 when $R_0 = 1$. The bifurcation parameter is the effective contact rate β.

Proof. We put $R_0 = 1$ and solve the equation for β and replace it by β_c Which is the bifurcation parameter. Therefore,

$$\beta_c = \frac{(\epsilon_1 + \epsilon_2 + \alpha + \mu)\left((\rho + \mu)(\nu_1 + \nu_2 + \mu) - \rho\nu_1\right)}{A(\nu_1 + \nu_2 + \mu)\left(1 + \frac{(\delta_1 + \delta_2 + \delta_3 + \mu)\,\alpha + \delta_2\epsilon_2}{(\zeta + \gamma + \mu + \mu_o)\,(\delta_1 + \delta_2 + \delta_3 + \mu) - \delta_2\zeta}\right)}$$

The Jacobian matrix of the system evaluated at the disease-free equilibrium P_0 is given by:

$$J_{P_0} = \begin{pmatrix} -(\rho+\mu) & -\beta_c S_0 & -\beta_c S_0 & \delta_3 & \upsilon_1 & \tau \\ 0 & \beta_c S_0 - Z_1 & \beta_c S_0 & 0 & 0 & 0 \\ 0 & \alpha & -Z_2 & \delta_2 & \upsilon_2 & 0 \\ 0 & \varepsilon_2 & \zeta & -Z_3 & 0 & 0 \\ \rho & \varepsilon_1 & 0 & 0 & -Z_4 & 0 \\ 0 & 0 & \gamma & \delta_1 & 0 & -Z_5 \end{pmatrix}$$

Applying row operations and determinant expansion, the matrix reduces to the following 4×4 form:

$$J_{p_0} = \begin{pmatrix} \beta S_0 - Z_1 & \beta S_0 & 0 & 0 \\ \alpha & -Z_2 & \delta_2 & \upsilon_2 \\ \varepsilon_2 & \zeta & -Z_3 & 0 \\ \varepsilon_1 - \dfrac{\rho\beta S_0}{\rho+\mu} & \dfrac{\rho}{\rho+\mu}\left(-\beta S_0 + \dfrac{\gamma\tau}{Z_5}\right) & \dfrac{\rho}{\rho+\mu}\left(\delta_3 + \dfrac{\delta_1\tau}{Z_5}\right) & -Z_4 + \dfrac{\rho\upsilon_1}{\rho+\mu} \end{pmatrix}$$

The characteristic polynomial is

$$\lambda^4 + a_1\lambda^3 + a_2\lambda^2 + a_3\lambda + a_4 = 0$$

where

$$\begin{aligned} a_4 = {} & (\beta S_0 - Z_1)\left[\frac{\rho}{\rho+\mu}\left(-\beta S_0 + \frac{\gamma\tau}{Z_5}\right)\upsilon_2 Z_3 - \frac{\rho}{\rho+\mu}\left(\delta_3 + \frac{\delta_1\tau}{Z_5}\right)\upsilon_2\zeta\right] \\ & - \beta S_0\left[\left(\varepsilon_1 - \frac{\rho\beta S_0}{\rho+\mu}\right)\upsilon_2 Z_3 + \frac{\rho}{\rho+\mu}\left(\delta_3 + \frac{\delta_1\tau}{Z_5}\right)\upsilon_2\varepsilon_2\right] \\ & + Z_1(Z_2Z_3 - \delta_2\zeta)\left(-Z_4 + \frac{\rho\upsilon_1}{\rho+\mu}\right)(R_0 - 1) \end{aligned}$$

The bifurcation point occurs when the constant term satisfies

$$a_4 = 0$$

Solving $a_4 = 0$ for β yields the critical contact rate $\beta = \beta_c$ corresponding to $R_0 = 1$.

4.1. Direction of Bifurcation

The Jacobian matrix of the system at the disease-free equilibrium point P_0 is given by

$$J_{P_0} = \begin{pmatrix} -(\rho+\mu) & -\beta_c S_0 & -\beta_c S_0 & \delta_3 & \upsilon_1 & \tau \\ 0 & \beta_c S_0 - Z_1 & \beta_c S_0 & 0 & 0 & 0 \\ 0 & \alpha & -Z_2 & \delta_2 & \upsilon_2 & 0 \\ 0 & \varepsilon_2 & \zeta & -Z_3 & 0 & 0 \\ \rho & \varepsilon_1 & 0 & 0 & -Z_4 & 0 \\ 0 & 0 & \gamma & \delta_1 & 0 & -Z_5 \end{pmatrix}$$

To apply the center manifold theory, we first compute the right eigenvector m and the left eigenvector v corresponding to the zero eigenvalue of J_{P_0}.

The right eigenvector satisfies the equation

$$J_{P_0} m = \begin{pmatrix} 0 \\ 0 \\ 0 \\ 0 \\ 0 \\ 0 \end{pmatrix}$$

That is,

$$\begin{pmatrix} -(\rho+\mu) & -\beta_c S_0 & -\beta_c S_0 & \delta_3 & \upsilon_1 & \tau \\ 0 & \beta_c S_0 - Z_1 & \beta_c S_0 & 0 & 0 & 0 \\ 0 & \alpha & -Z_2 & \delta_2 & \upsilon_2 & 0 \\ 0 & \varepsilon_2 & \zeta & -Z_3 & 0 & 0 \\ \rho & \varepsilon_1 & 0 & 0 & -Z_4 & 0 \\ 0 & 0 & \gamma & \delta_1 & 0 & -Z_5 \end{pmatrix} \begin{pmatrix} m_1 \\ m_2 \\ m_3 \\ m_4 \\ m_5 \\ m_6 \end{pmatrix} = \begin{pmatrix} 0 \\ 0 \\ 0 \\ 0 \\ 0 \\ 0 \end{pmatrix}$$

Solving, we obtain:

$$m_2 = \frac{\rho\upsilon_2}{Z_4\mathcal{C}}\ m_1,$$

$$m_3 = \frac{Z_1 - \beta_c S_0}{\beta_c S_0} m_2 = \frac{(Z_1 - \beta_c S_0)\rho\upsilon_2}{\beta_c S_0 Z_4 C} m_1,$$

$$m_4 = \frac{\varepsilon_2 m_2 + \zeta m_3}{Z_3} = \frac{[\beta_c S_0 \varepsilon_2 - \zeta(\beta_c S_0 - Z_1)]\rho\upsilon_2}{\beta_c S_0 Z_3 Z_4\, \mathcal{C}} m_1,$$

$$m_5 = \frac{\rho m_1 + \varepsilon_1 m_2}{Z_4} = \frac{\rho}{Z_4} m_1 + \frac{\varepsilon_1 \rho \upsilon_2}{Z_4^2 C} m_1,$$

$$m_6 = \frac{\gamma m_3 + \delta_1 m_4}{Z_5} = \frac{1}{Z_5}\left[\gamma\left(\frac{Z_1 - \beta_c S_0}{\beta_c S_0}\right) + \delta_1\left(\frac{\beta_c S_0 \varepsilon_2 - \zeta(\beta_c S_0 - Z_1)}{\beta_c S_0 Z_3}\right)\right] \frac{\rho\upsilon_2}{Z_4\mathcal{C}} m_1$$

where

$$C = \frac{Z_2(Z_1 - \beta_c S_0)}{\beta_c S_0} - \alpha - \delta_2 \frac{\beta_c S_0 \varepsilon_2 - \zeta(\beta_c S_0 - Z_1)}{\beta_c S_0 Z_3} - \frac{\upsilon_2 \varepsilon_1}{Z_4}$$

Similarly, the left eigenvector satisfies

$$v^\top J_{P_0} = \mathbf{0}^\top$$

That is,

$$\begin{pmatrix} v_1 \\ v_2 \\ v_3 \\ v_4 \\ v_5 \\ v_6 \end{pmatrix}^\top \begin{pmatrix} -(\rho+\mu) & -\beta_c S_0 & -\beta_c S_0 & \delta_3 & \upsilon_1 & \tau \\ 0 & \beta_c S_0 - Z_1 & \beta_c S_0 & 0 & 0 & 0 \\ 0 & \alpha & -Z_2 & \delta_2 & \upsilon_2 & 0 \\ 0 & \varepsilon_2 & \zeta & -Z_3 & 0 & 0 \\ \rho & \varepsilon_1 & 0 & 0 & -Z_4 & 0 \\ 0 & 0 & \gamma & \delta_1 & 0 & -Z_5 \end{pmatrix} = \begin{pmatrix} 0 \\ 0 \\ 0 \\ 0 \\ 0 \\ 0 \end{pmatrix}^\top$$

Solving, we get:

$$v_1 = v_1 \quad \text{(free parameter)},$$

$$v_2 = \frac{\beta_c S_0 v_1 - \alpha v_3 - \varepsilon_2 v_4 - \varepsilon_1 v_5}{\beta_c S_0 - Z_1},$$

$$v_3 = \frac{Z_4(\rho+\mu) - v_1\rho}{v_2\rho}\, v_1,$$

$$v_4 = \left[\frac{\delta_3}{Z_3} + \frac{\delta_2 Z_4(\rho+\mu) - v_1\rho}{v_2\rho Z_3} + \frac{\delta_1\tau}{Z_5 Z_3}\right] v_1,$$

$$v_5 = \frac{\rho+\mu}{\rho}\, v_1, v_6 = \frac{\tau}{Z_5}\, v_1$$

We define the nonlinear functions of the system as follows:

$$g_1 = A - \beta_c S(E+I) - (\rho+\mu)S + \delta_3 Q + v_1 V + \tau R$$

$$g_2 = \beta_c S(E+I) - Z_1 E$$

$$g_3 = \varepsilon_2 E + \zeta I - Z_3 Q$$

$$g_4 = \alpha E - Z_2 I + \delta_2 Q + v_2 V$$

$$g_5 = \rho S + \varepsilon_1 E - Z_4 V$$

$$g_6 = \gamma I + \delta_1 Q - Z_5 R$$

Only the functions g_1 and g_2 are used, since the corresponding components v_1, v_2 of the left eigenvector are non-zero.

The second-order partial derivatives needed are:

$$\frac{\partial^2 g_1}{\partial S \partial E} = \frac{\partial^2 g_1}{\partial S \partial I} = -\beta_c, \quad \frac{\partial^2 g_2}{\partial S \partial E} = \frac{\partial^2 g_2}{\partial S \partial I} = \beta_c$$

$$\frac{\partial^2 g_2}{\partial E \partial \beta_c} = \frac{\partial^2 g_2}{\partial I \partial \beta_c} = S_0, \quad \frac{\partial^2 g_1}{\partial S \partial \beta_c} = 0$$

The bifurcation coefficients are calculated as

$$a = \sum_{i,j,k=1}^{6} v_k m_i m_j \frac{\partial^2 g_k}{\partial x_i \partial x_j}, \quad b = \sum_{i,k=1}^{6} v_k m_i \frac{\partial^2 g_k}{\partial x_i \partial \beta_c}$$

Substituting into the expressions gives:

$$a = \Big[v_1\big(m_1 m_2 \tfrac{\partial^2 g_1}{\partial S \partial E} + m_1 m_3 \tfrac{\partial^2 g_1}{\partial S \partial I}\big) + v_2\big(m_1 m_2 \tfrac{\partial^2 g_2}{\partial S \partial E} + m_1 m_3 \tfrac{\partial^2 g_2}{\partial S \partial I}\big)\Big]$$

$$= \Big[v_1(-\beta_c m_1(m_2+m_3)) + v_2(\beta_c m_1(m_2+m_3))\Big]$$

$$= (v_2 - v_1)\, m_1 \beta_c (m_2 + m_3)$$

Evaluation of b. Only g_2 contributes, hence

$$b = v_2\Big(m_2 \tfrac{\partial^2 g_2}{\partial E \partial \beta_c} + m_3 \tfrac{\partial^2 g_2}{\partial I \partial \beta_c}\Big)$$

$$= v_2 S_0 (m_2 + m_3)$$

$$a = (v_2 - v_1)(m_2+m_3)\beta_c m_1, b = v_2 S_0 (m_2 + m_3)$$

Where m_1, m_2, m_3 and v_1, v_2 are components of the right and left eigenvectors associated with the zero eigenvalue. Since the signs satisfy:

$$a > 0, (v_2 > v_1) \quad \text{and} \quad b > 0$$

The system undergoes a **Forward (supercritical) bifurcation** at the critical threshold $\mathcal{R}_0 = 1$. This implies that when $\mathcal{R}_0 < 1$, the disease-free equilibrium is locally asymptotically stable. As $\mathcal{R}_0$ increases beyond 1, a locally stable endemic equilibrium emerges smoothly.

5. Sensitivity Analysis of R_0

The normalized forward sensitivity indices measure the relative change in the basic reproduction number R_0 with respect to a relative change in each parameter. Using these indices, we figure out the most influential parameters that are responsible for the disease transmission and control. To perform sensitivity analysis, we use the formula given by

$$\Upsilon_x^{R_0} = \frac{\partial R_0}{\partial x} \times \frac{x}{R_0}$$

$$\Upsilon_\beta^{R_0} = \Upsilon_A^{R_0} = 1$$

$$\Upsilon_{\epsilon_1}^{R_0} = -\frac{\epsilon_1}{\epsilon_1 + \epsilon_2 + \alpha + \mu}, \quad \Upsilon_\alpha^{R_0} = -\frac{\alpha}{\epsilon_1 + \epsilon_2 + \alpha + \mu} + \frac{\alpha}{D_1 D}$$

$$\Upsilon_{\epsilon_2}^{R_0} = -\frac{\epsilon_2}{\epsilon_1 + \epsilon_2 + \alpha + \mu} + \frac{\delta_2}{D_1 D}$$

$$\Upsilon_{\nu_1}^{R_0} = \frac{(\rho + \mu)(\nu_1 + \nu_2 + \mu) - \rho\mu}{(\rho + \mu)(\nu_1 + \nu_2 + \mu) - \rho\nu_1} - 1$$

$$\Upsilon_{\nu_2}^{R_0} = \frac{(\rho + \mu)(\nu_1 + \nu_2 + \mu)}{(\rho + \mu)(\nu_1 + \nu_2 + \mu) - \rho\nu_1}$$

$$\Upsilon_{\delta_2}^{R_0} = \frac{\epsilon_2}{D_1 D} - \frac{\zeta}{D}, \quad \Upsilon_\zeta^{R_0} = \frac{I - \delta_2}{D}, \quad \Upsilon_\gamma^{R_0} = \frac{1}{D}, \quad \Upsilon_{\mu_o}^{R_0} = \frac{1}{D}$$

$$\Upsilon_\mu^{R_0} = 1 - \frac{\mu}{\epsilon_1 + \epsilon_2 + \alpha + \mu} - \frac{\mu\left((\nu_1 + \nu_2 + \rho) + 2\mu\right)}{(\rho + \mu)(\nu_1 + \nu_2 + \mu) - \rho\nu_1} + \frac{\mu\alpha D - \mu\left((D_1)\alpha + \delta_2\epsilon_2\right) D'}{D^2}$$

where

$$D = (\zeta + \gamma + \mu + \mu_o)(D_1) - \delta_2\zeta$$

$$D_1 = (\delta_1 + \delta_2 + \delta_3 + \mu), \quad D' = (D_1 + 1)(\zeta + \gamma + \mu + \mu_o + 1)$$

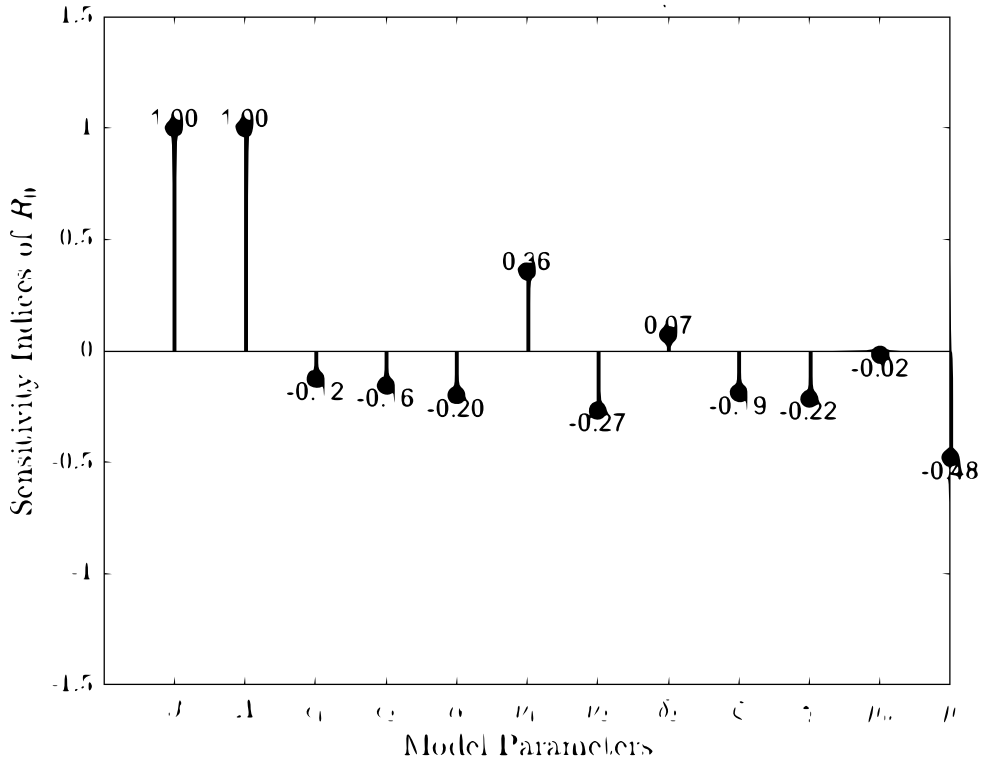

Figure 3: Normalized Forward Sensitivity indices

6. Numerical simulation

To validate the theoretical results obtained from the bifurcation analysis, we perform numerical simulations of the proposed model system using the parameter values. The numerical solutions are generated by solving the system of differential equations (1) using the ODE solver method in Python.

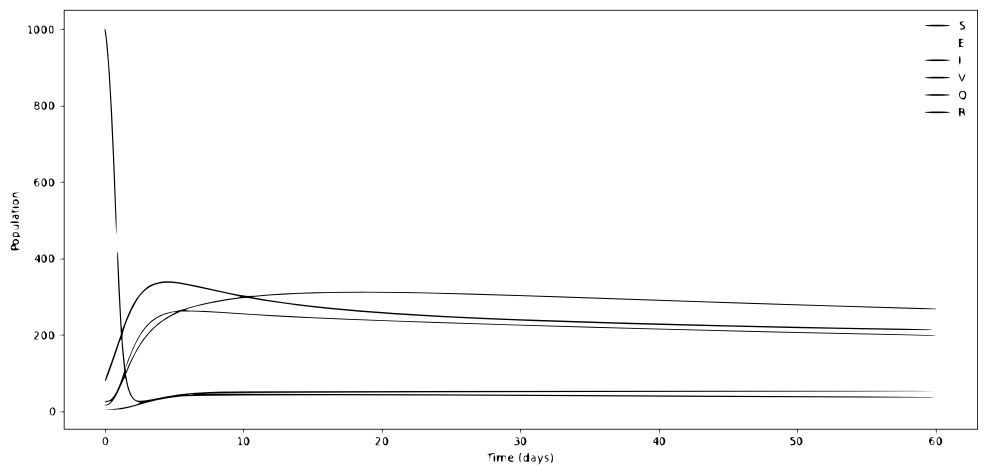

Figure 4: SEIVQR Model:All Compartments in one graph

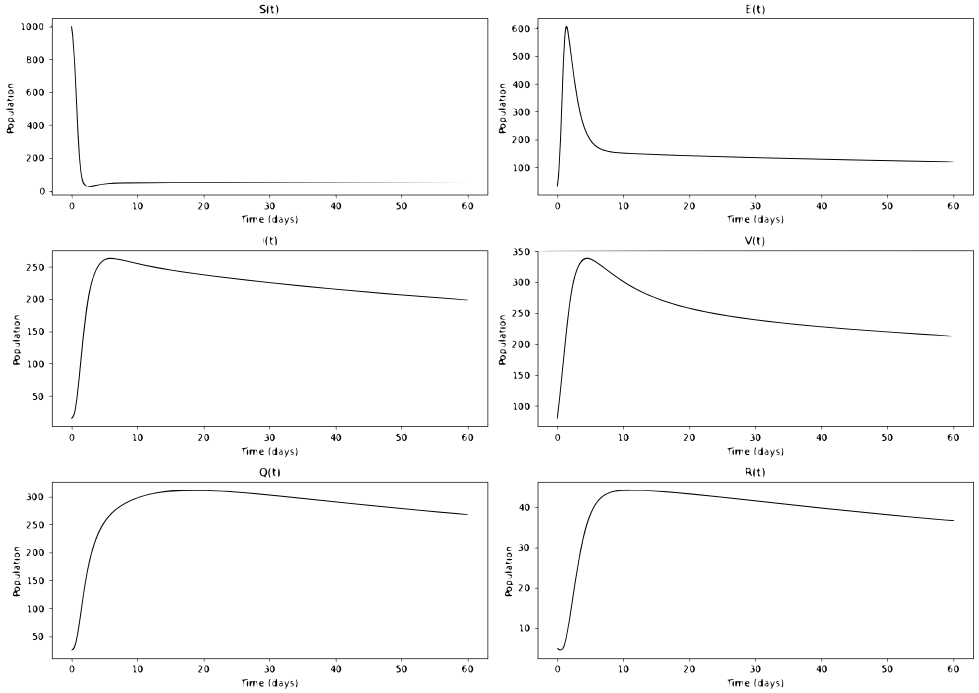

Figure 5: SEIVQR Model:Separate graphs for each compartment

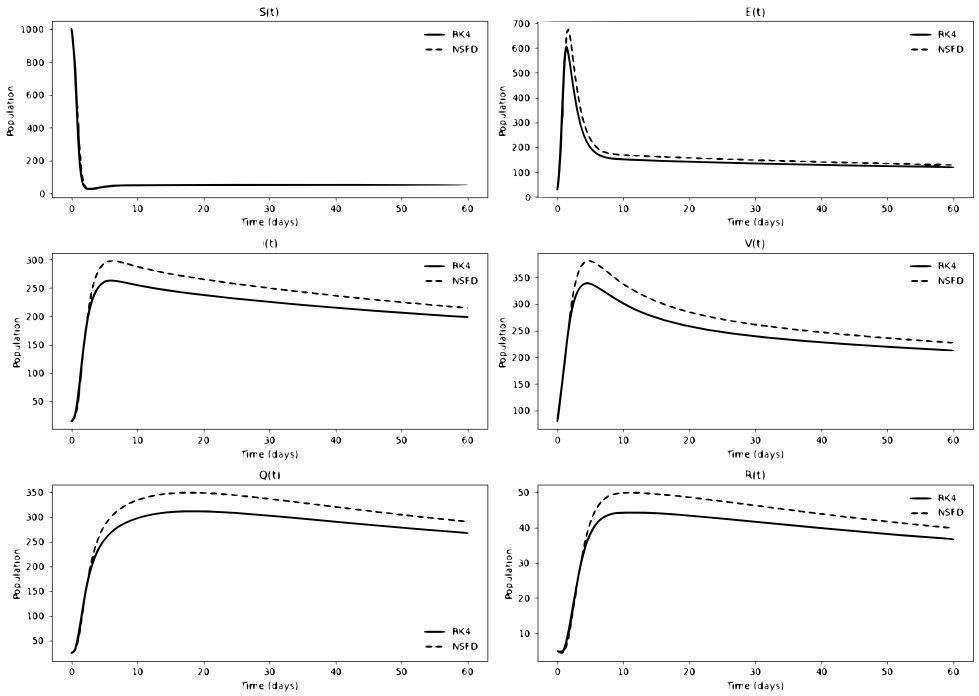

Figure 6: SEIVQR Model:RK4 vs NSFD for all compartments

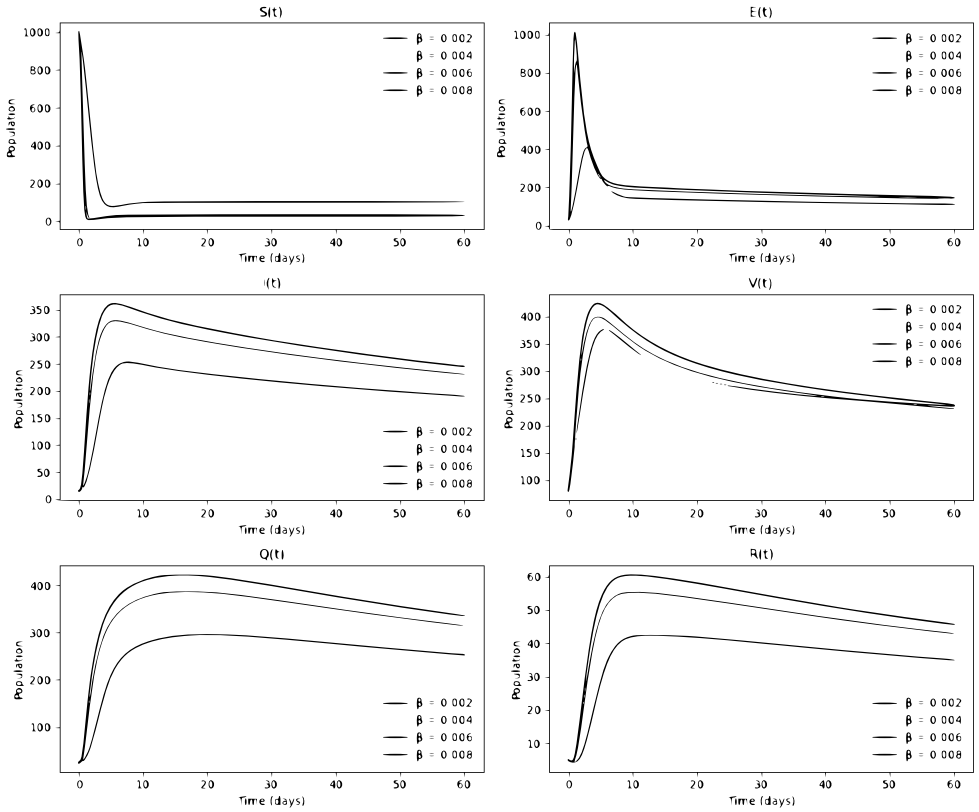

Figure 7: SEIVQR Model:NSFD multigraphs with varying β

7. Discussion

Figure 4 illustrates the SEIVQR model simulation, which highlights the temporal dynamics of each compartment involved in the progression of the illness. Susceptible (S), Exposed (E), Infectious (I), Vaccinated (V), Quarantined (Q), and Recovered (R) are the six compartments that are displayed together in the combined graph to emphasize their overall interactions. Rapid initial transmission is indicated by the reported significant reduction in the susceptible population at beginning of the outbreak. A brief incubation and infectious phase is suggested by the discernible peaks that follow in the exposed and infectious compartments.

Control measures like immunization and quarantine start to take center stage as the system develops. At first, there are increasing trends in the quarantined and vaccinated compartments, which helps to lower the number of new infections. The restored population steadily grows, reflecting the community's slow build-up of immunity.

Figure 5 presents each population separately in its corresponding compartment graph, thereby offering a clearer illustration of its dynamic behavior. Early peaks followed by slow reductions are shown in the infectious and exposed classes, indicating how well containment and recovery procedures worked. As susceptible individuals are reduced, the vaccinated compartment gradually decreases or plateaus after first increasing as a result of immunization efforts. While the recovered class expands consistently over time, indicating effective case resolution, the quarantined group grows quickly and stabilizes.

Overall, the dynamics demonstrate that a robust vaccine and quarantine response can dramatically change the course of an epidemic, resulting in a contained outbreak and long-term disease prevention.

In Figure 6, the numerical behavior of the SEIVQR model's compartments over time shows clear differences between the NSFD (Nonstandard Finite Difference) scheme and the RK4 (Runge–Kutta 4^{th} order) technique. Both approaches preserve the overall qualitative trends of disease progression; however, the NSFD scheme provides more stable and biologically consistent results, particularly for longer

simulation times. In contrast, the RK4 method, due to its fixed step size and accumulated numerical drift, may display slight oscillations around equilibrium values. For example, the NSFD approach maintains smooth decline and convergence in the susceptible and recovered populations, while RK4 exhibits minor fluctuations. Similarly, NSFD more accurately captures the saturation and stabilization of disease dynamics in the exposed and infected compartments. These findings demonstrate that the NSFD scheme preserves the boundedness and positivity properties of epidemiological models more effectively, making it a reliable tool for analyzing long-term dynamics in compartmental systems.

In Figure 7, with all other parameters and initial conditions fixed at $S(0) = 1000$, $E(0) = 30$, $I(0) = 15$, $V(0) = 80$, $Q(0) = 25$, and $R(0) = 5$, the multigraphs display the dynamics of the SEIVQR model under the NSFD scheme for$\beta \in 0.002, 0.004, 0.006, 0.008$. As expected, raising β accelerates the spread of the illness, leading to an earlier and higher peak in the infectious (I) and exposed (E) populations. Due to faster transmission, this also causes a more noticeable decline in the susceptible (S) group. Due to transitions from other states, the quarantined (Q) and vaccinated (V) compartments respond with moderate growth, whereas the recovered (R) population accumulates more quickly with larger β values. The results show the need of regulating contact rates in epidemic situations by demonstrating how sensitive disease progression is to the rate of transmission.

8. Conclusion

In this study, we developed and analyzed a novel six-compartment SEIVQR deterministic model for Mpox transmission that explicitly integrates both vaccination and quarantine strategies. Unlike many existing Mpox models that consider only vaccination or basic SEIR dynamics, our framework simultaneously captures the joint impact of immunization programs and isolation measures on disease progression. This dual focus represents a key novelty of our work, as it reflects realistic intervention policies that were implemented during the 2022–2023 Mpox outbreaks.

Using the next-generation matrix approach, we derived the basic reproduction number R_0 and rigorously established the local and global stability conditions of both disease-free and endemic equilibria. Our bifurcation analysis via center manifold theory revealed that the system undergoes a forward bifurcation at $R_0 = 1$, highlighting that reducing R_0 below unity is both necessary and sufficient for disease elimination. Numerical simulations, carried out using the Nonstandard Finite Difference (NSFD) method, validated the theoretical results and further demonstrated the advantages of NSFD in preserving positivity and biological consistency over standard RK4.

The findings emphasize the importance of coordinated strategies: reducing the transmission rate (β), enhancing quarantine implementation (ζ), and increasing vaccination coverage (ρ) are shown to be the most effective levers for Mpox control. By quantifying the interplay between these interventions, our model provides public health authorities with a rigorous analytical tool for evaluating and optimizing control measures.

For future research, rather than only adding stochasticity or delays in a generic sense, we suggest three concrete directions emerging from the current limitations: (i) incorporating contact heterogeneity to account for sexual vs. non-sexual transmission pathways, since our assumption of homogeneous mixing may oversimplify real outbreaks, (ii) fitting the model to recent outbreak datasets to validate parameter estimates and intervention thresholds, and (iii) extending the framework to include waning vaccine immunity over longer time horizons, which was identified as a sensitive parameter in our stability analysis. Addressing these gaps would further strengthen the applicability of the model for predictive and policy-oriented purposes.

Acknowledgments

We think the referee by your suggestions.

References

1. Thornhill, J.P., Gandhi, M. and Orkin, C., 2024. Mpox: the reemergence of an old disease and inequities. Annual Review of Medicine, 75(1), pp.159-175.

2. World Health Organization, 2024. *WHO declares Mpox a global health emergency*. [online] Available at: https://www.verywellhealth.com/mpox-who-global-health-emergency-2024-8696238 [Accessed 6 Aug. 2025].

3. Meo, M.O., Meo, M.Z., Khan, I.M., Butt, M.A., Usmani, A.M. and Meo, S.A., 2024. Rising epidemiological trends in prevalence and mortality of mpox: Global insights and analysis. Saudi Medical Journal, 45(12), p.1334.

4. Reuters, 2024. Cluster of drug-resistant mpox identified in five states, US officials report. [online] Available at: https://www.reuters.com/business/healthcare-pharmaceuticals/cluster-drug-resistant-mpox-identified-five-states-us-officials-report-2024-10-10/ [Accessed 6 Aug. 2025].

5. Sahra, S., Villalobos, R.O., Scott, B.M., Bowman, D.J., Sassine, J., Salvaggio, M., Drevets, D.A. and Higuita, N.I.A., 2023. The diagnostic dilemma for atypical presentation of progressive human Mpox. BMC Infectious Diseases, 23(1), p.850.

6. Kularathne, Y., Janitha, P. and Ambepitiya, S., 2024. Mpox Screen Lite: AI-Driven On-Device Offline Mpox Screening for Low-Resource African Mpox Emergency Response. arXiv preprint arXiv:2409.03806.

7. Yue, Y., Xue, J., Liang, H., Li, Z. and Wang, Y., 2025, April. MpoxMamba: A Grouped Mamba-based Lightweight Hybrid Network for Mpox Detection. In ICASSP 2025-2025 IEEE International Conference on Acoustics, Speech and Signal Processing (ICASSP) (pp. 1-5). IEEE.

8. Cao, X., Ye, W., Moise, K. and Coffee, M., 2024. MpoxVLM: A Vision-Language Model for Diagnosing Skin Lesions from Mpox Virus Infection. arXiv preprint arXiv:2411.10888.

9. Malik, S., Ahmad, T., Ahsan, O., Muhammad, K. and Waheed, Y., 2023. Recent developments in mpox prevention and treatment options. Vaccines, 11(3), p.500.

10. Zhai, Y., Han, Y., Wang, W. and Tan, W., 2025. Advancements in Mpox vaccine development: A comprehensive review of global progress and recent data. Biomedical and Environmental Sciences, 38(2), pp.248-254.

11. Yue, Y., Jiang, M., Zhang, X., Xu, J., Ye, H., Zhang, F., Li, Z. and Li, Y., 2024. Mpox-AISM: AI-mediated super monitoring for mpox and like-mpox. Iscience, 27(5).

12. Bapolisi, W.A., Krasemann, S., Wayengera, M., Kirenga, B., Bahizire, E., Malembaka, E.B., Fodjo, J.N.S., Colebunders, R. and Katoto, P.D., 2024. Mpox outbreak—tecovirimat resistance, management approaches, and challenges in HIV-endemic regions. The Lancet Infectious Diseases, 24(11), pp.e672-e673.

13. World Health Organization, 2024. 2023–2025 mpox epidemic. [online] Available at: https://en.wikipedia.org/wiki/2023%E2%80%932025_mpox_epidemic [Accessed 6 Aug. 2025].

14. Jadhav, V., Paul, A., Trivedi, V., Bhatnagar, R., Bhalsinge, R. and Jadhav, S.V., 2025. Global epidemiology, viral evolution, and public health responses: a systematic review on Mpox (1958–2024). Journal of Global Health, 15, p.04061.

15. Hassan, O.A., Olaniyi, S.O., Alzahrani, E. and Khan, M.A., 2023. Mathematical analysis of the spread of monkeypox using a deterministic model. *Frontiers in Applied Mathematics and Statistics*, 9. https://doi.org/10.3389/fams.2023.1111615.

16. Elaiw, A.M., *et al.*, 2021. A Mathematical Model for Stability Analysis of Covid-like Epidemic. *medRxiv*. https://doi.org/10.1101/2021.05.25.21257853.

17. Ahmad, I., Hussain, F., Mlaiki, N., Ali, N., Ullah, Z., EID, A.A. and Fatima, N., 2025. Stability and Bifurcation Analysis of an Epidemic Model for Ebola Virus Dynamics with Control Strategies. Fractals, p.2540161.

18. Ullah, I., Ahmad, I., Ali, N., Haq, I.U., Idrees, M., Albalwi, M.D. and Yavuz, M., 2024. Mathematical modeling and analysis of Ebola virus disease dynamics: implications for intervention strategies and healthcare resource optimization. Mathematical and Computational Applications, 29(5), p.94.

19. Ullah, I., Ahmad, I., Ali, N., Ahmad, H. and Haq, I.U., 2024. Mathematical modeling and analysis of dynamics of* Neisseria Gonorrhea* disease with self protection, treatment and natural immunity. Global Journal of Sciences, 1(1), pp.40-55.

20. Younas, H., Ahmad, I., Ali, N., Haq, I.U., Albalwi, M.D., Muhammad, S. and Shuaib, M., 2024. Modeling rabies dynamics: the impact of vaccination and infectious immigrants on public health. Contemporary Mathematics, pp.3255-3279.

21. Ullah, I., Ali, N., Haq, I.U., Ahmad, I., Albalwi, M.D. and Ali Biswas, M.H., 2024. Analysis of COVID-19 Disease Model: Backward Bifurcation and Impact of Pharmaceutical and Nonpharmaceutical Interventions. International Journal of Mathematics and Mathematical Sciences, 2024(1), p.6069996.

22. Khan, T., Ullah, R., Zaman, G. and Ahmad, I., 2021. The analysis of hepatitis B virus (HBV) transmission using an epidemic model. Natural and Applied Sciences International Journal (NASIJ), 2(1), pp.70-79.

23. Diyar, R., Ahmad, I., Ali, N., Haq, I.U., Idrees, M. and Albalwi, M.D., 2024. A fractional order mathematical model for the omicron: a new variant of COVID-19. Physica Scripta, 99(11), p.115255.

24. ul Haq, I., Ali, N., Ahmad, H., Sabra, R., Albalwi, M.D. and Ahmad, I., 2025. Mathematical analysis of a coronavirus model with Caputo, Caputo–Fabrizio–Caputo fractional and Atangana–Baleanu–Caputo differential operators. International Journal of Biomathematics, 18(01), p.2350085.

25. Khan, M., Khan, T., Ahmad, I., Shah, Z. and Khan, A., 2022. Modeling of Hepatitis B virus transmission with fractional analysis. Mathematical Problems in Engineering, 2022(1), p.6202049.

26. Vanderbauwhede, A. and Iooss, G., 1992. Center manifold theory in infinite dimensions. In Dynamics reported: expositions in dynamical systems (pp. 125-163). Berlin, Heidelberg: Springer Berlin Heidelberg.

27. Castillo-Chavez, C. and Song, B., 2004. Dynamical models of tuberculosis and their applications. Math. Biosci. Eng, 1(2), pp.361-404.

28. Ward, T., Christie, R., Paton, R.S., Cumming, F. and Overton, C.E., 2022. Transmission dynamics of monkeypox in the United Kingdom: contact tracing study. bmj, 379.

29. Jan, M.N., Zaman, G., Ali, N., Ahmad, I. and Shah, Z., 2022. Optimal control ap- plication to the epidemiology of HBV and HCV co-infection. International Journal of Biomathematics, 15(03), p.2150101.

30. Zafar, Z.U.A., Shah, Z., Ali, N., Kumam, P. and Alzahrani, E.O., 2020. Numerical study and stability of the Lengyel–Epstein chemical model with diffusion. Advances in Difference Equations, 2020(1), p.427.

31. Jan, M.N., Ali, N., Zaman, G., Ahmad, I., Shah, Z. and Kumam, P., 2020. HIV-1 infec- tion dynamics and optimal control with Crowley-Martin function response. Computer Methods and Programs in Biomedicine, 193, p.105503.

Ibrar Ul Haq, Imtiaz Ahmad, Nigar. Ali
Department of Mathematics,
University of Malakand,
Chakdara Dir(Lower),18000,Khyber Pakhtunkhwa, Pakistan.
E-mail address: uibrar734@gmail.com, iahmaad@hotmail.com, nigaruom@gmail.com

and

Nasro Min-Allah
Department of Computer Science,
College of Computer Science and Information Technology,
Imam Abdulrahman Bin Faisal University,
P.O. Box 1982, Dammam, 31441, Saudi Arabia
E-mail address: nabdullatief@iau.edu.sa

and

Amna
Department of Mathematics,
Women University Swabi,
KP, Pakistan
E-mail address: amnayousafzai710@gmail.com

and

Saeed Islam
Department of Mechanical Engineering,
Prince Mohammad Bin Fahd University,
Al-Khobar, 31952, Saudi Arabia
E-mail address: sislam@pmu.edu.sa

and

Ishtiaq Ali,
Dept of Mathematics and Statistics,
Al-Ahsa, 31942, King Faisal University,
Saudi Arabia
E-mail address: iamirzada@kfu.edu.sa